Kidney International, Vol. 44 (1993), pp. 985–996

Quantification and parametric imaging of renal cortical blood flow *in vivo* based on Patlak graphical analysis

EGBERT U. NITZSCHE, YONG CHOI, DAVID KILLION, CARL K. HOH, RANDALL A. HAWKINS, J. THOMAS ROSENTHAL, DENIS B. BUXTON, SUNG-CHENG HUANG, MICHAEL E. PHELPS, and HEINRICH R. SCHELBERT

Division of Nuclear Medicine and Biophysics, Division of Urology, and Division of Nephrology, UCLA School of Medicine, Los Angeles, California, USA

Quantification and parametric imaging of renal cortical blood flow *in vivo* based on Patlak graphical analysis. Patlak graphical analysis was applied to quantify renal cortical blood flow with N-13 ammonia and dynamic positron emission tomography. Measurements were made in a swine model of kidney transplantation with a wide range of normal and abnormal renal blood flows ($N = 57$ studies) and in 20 healthy human volunteers ($N = 45$ studies). Estimates of renal cortical blood flow by the Patlak method were compared to those from a two-compartment model for N-13 ammonia. In addition, estimates of renal cortical blood flow by the N-13 ammonia PET approach were compared in 10 normal human volunteers to estimates by the metabolically inert, freely diffusible O-15 water and a one-compartment model. Patlak graphical analysis estimates of renal cortical blood flow correlated linearly with the standard two-compartment model in pigs ($y = -0.05 + 1.01x$, $r = 0.99$) and in humans ($y = 0.57 + 0.88x$, $r = 0.93$). Estimates of renal cortical blood flow by O-15 water in human volunteers were also linearly correlated with those by N-13 ammonia and the Patlak graphical analysis ($y = 0.71 + 0.84x$, $r = 0.86$). Renal cortical blood flow estimates were highly reproducible both with N-13 ammonia and O-15 water measurements in humans. It is concluded that the Patlak graphical analysis with N-13 ammonia dynamic positron emission tomographic imaging renders accurate and reproducible estimates of renal cortical blood flow. Moreover, the graphical analysis approach is 1,000 times faster than the standard model fitting approach and suitable for generating parametric images of renal blood flow in the clinical setting.

Experimental studies have shown renal blood flow (RBF) to be heterogeneous under physiologic, ischemic and hyperemic conditions. This heterogeneity has been demonstrated in animal models of clinically important conditions such as trauma, hemorrhage and shock [1]. In addition to the major renal arteries and veins and their related subbranches, there are several distinct microvascular networks: the glomerular and the cortical peritubular microcirculations and microcirculatory systems that supply and drain the medulla. Methods for measuring RBF have not been widely applied clinically because of their invasiveness, technical complexity [2], and limited clinical availability. Additionally, no clear correlation between the distribution of intrarenal blood flow and renal function has been established [3].

A noninvasive imaging method that provides absolute quantitative estimates of RBF per unit mass of renal tissue in humans is of potential investigative and clinical utility. For example, abnormalities in RBF resulting from advanced arterial hypertension, acute cortical necrosis, acute tubular necrosis, acute rejection of a kidney transplant or cyclosporine toxicity could potentially be defined more quantitatively and, thus, objectively.

Positron emission tomography (PET) permits quantitative volumetric measurements of tissue radioactivity concentrations from cross sectional images. Chen et al [4] demonstrated in dog experiments that N-13 ammonia dynamic imaging with PET provides accurate estimates of renal cortical blood flow (RCBF). They estimated RCBF by fitting the regional cortical time-activity curves to a two-compartment model for N-13 ammonia. The estimates by this approach correlated well with independent measurements by the radiolabeled microsphere and arterial sample technique.

N-13 ammonia has longer tissue retention times and offers better count statistics than other PET flow tracers such as O-15 water. However, retention of N-13 ammonia in tissue may be sensitive to metabolic alterations. Further, its extraction fraction declines with increasing RBF. Although validated in dogs, the validity of the N-13 ammonia PET approach for quantifying RCBF remains to be established in humans. This is because species related differences may alter the relationship between the first-pass retention fraction of N-13 ammonia and RBF. Moreover, quantification of RCBF with the two-compartment model is tedious, time consuming and, consequently, clinically impractical. This limitation could be overcome with a more simple and computationally efficient graphical analysis method [5, 6].

The purpose of this study was therefore to answer the following questions: (1) Do the kinetics of N-13 ammonia in the kidney satisfy the requirements of Patlak graphical analysis so that RCBF can be quantified more concisely? If the kinetics are indeed amenable to the graphical analysis, are the estimates of RCBF accurate? (2) Can accurate estimates of RCBF be obtained in humans with N-13 ammonia? and (3) Are such measurements reproducible?

Received for publication April 22, 1993
and in revised form June 22, 1993
Accepted for publication June 24, 1993

Methods

The study design includes studies in animals and in humans. The animal studies served to test the validity of the graphical analysis approach over a wide range of RCBF's as well as of normal and abnormal conditions. The validity of the measurement approach was then tested in humans and compared to an independent measurement of RCBF with the previously established O-15 water approach [7].

Animals

Ten young adult female Duroc farm pigs (body weight ranging 25 to 30 kg) were studied repeatedly under different experimental conditions. These included normal-baseline (8 pigs, 8 studies), acute tubular necrosis in autotransplanted kidneys submitted to different durations of warm ischemia [120 min, 150 min, 180 min (8 pigs, 23 studies)], acute rejection of renal heterotransplants (2 pigs, 5 studies), renal hypertrophy (4 pigs, 9 studies) and acute as well as chronic cyclosporine toxicity (6 pigs, 12 studies). Pathologic conditions were confirmed by biopsy. A total of 57 studies (average 6 studies per animal) with N-13 ammonia and dynamic PET were performed. Details of renal transplantation of the pig model have been reported by Yanaga et al [8]. These standardized conditions for hemodynamics and hydration were applied to all PET studies.

Humans

Twenty healthy human subjects (16 male, 4 female, mean age 29 years, ranging 18 to 54 years) were studied. None had a history of prior renal disease. Entrance criteria included normal heart rate, blood pressure, blood cell count, serum creatinine level, plasma sodium and urine analysis. A total of 45 PET measurements were performed in the 20 human volunteers. The first ten subjects had repeat measurements after a 60 minute delay (to allow for N-13 decay, $T_{1/2}$ = 9.8 min) to test the reproducibility of the method. Ten subjects were studied with both N-13 ammonia and O-15 water. In this group, five subjects had repeat O-15 water studies to evaluate the reproducibility of the O-15 water RCBF method. O-15 water studies were separated by 15 minutes (O-15 $T_{1/2}$ = 2 min).

All volunteers were prepared by drinking 500 ml water 60 minutes prior to the study and were instructed to empty the bladder immediately prior to the PET procedure.

The animal and human studies were approved by the UCLA Animal Research Committee and the UCLA Human Subject Protection Committee. Maintenance and care of the pigs was in compliance with the National Institutes of Health guidelines for use of laboratory animals. All human subjects signed written consent forms after the procedures had been fully explained.

Radiopharmaceuticals

The animals were intravenously injected over 30 seconds with N-13 ammonia (20 mCi diluted in 2 to 8 ml saline) while acquisition of the serial transaxial tomographic images was started. The human volunteers were injected with 20 mCi N-13 ammonia and (in ten subjects) 30 mCi O-15 water over 30 seconds into a peripheral vein while acquisition of the serial transaxial tomographic images was started. Both tracers were produced and synthesized as reported previously [9, 10].

PET imaging

After obtaining a 30-minute blank scan and a 20-minute transmission image for photon attenuation correction, both N-13 ammonia and O-15 water emission images were acquired on a Siemens/CTI Model 931/08-12 tomograph. This device records 15 image planes simultaneously. The axial field of view is 10.8 cm. Ultrasound guidance was used for adequate position of the kidneys in the tomograph's field of view. All subjects were imaged in the supine position.

For N-13 ammonia, the acquisition protocol included twelve 10 second, six 20 second and four 240 second frames in both humans and animals. For the O-15 water studies in humans, twelve 10 second, four 30 second and one 60 second frame were acquired. Cross sectional images for all studies were reconstructed employing a Shepp-Logan filter with a cut-off frequency of 0.30 mm^{-1}, yielding an in plane spatial resolution at the center of the plane of approximately 10 mm full-width half-maximum.

Input function

Serial arterial blood samples of 1 ml each were drawn every 10 seconds for the first two minutes after tracer injection to measure directly the N-13 ammonia and O-15 water arterial input functions. N-13 and O-15 whole blood activity concentrations in pre-weighed tubes were measured in a well counter. In addition, for the N-13 ammonia studies, three whole blood samples (1 ml each) were drawn at 0.65 ± 0.06, 1.35 ± 0.08 and 2 ± 0.05 minutes after tracer injection to determine the time-dependent distribution of N-13 label between ammonia and its metabolites in the arterial input function as described previously [11]. These distribution measures were used to correct the arterial input function for the true amount of N-13 ammonia delivered to the kidneys.

Conversion factor between image data and well counter data

A cylinder phantom containing Ge-68/Ga-68 solution was scanned after each study in order to determine a conversion factor between image data in units of counts/pixel/sec and well counter data in units counts/ml/sec. This conversion factor was derived as follows: a known aliquot from the solution in the phantom was removed and its activity concentration measured in a well counter (Turn-Key Microsphere Measurement System, MICRAD). The calibration factor was derived from the ratio of counts/ml/sec measured in the well counter to the counts/pixel/sec recorded from the cylinder with the PET scanner.

Data analysis and applied corrections

Circular regions of interest (ROI) were drawn over the renal cortex using summed images (for example summing the dynamically acquired images one to twelve corresponding to time zero to two min post-injection). The ROI's encompassed the entire transaxial area of the cortex (one region per slice). The central area, including the renal medulla and collecting system, was omitted. The ROI's were then copied to the dynamic image set. Counts/pixel obtained from these ROI's were converted to counts/pixel/min by normalizing for the acquisition time of each dynamically acquired image. These values were then converted to equivalent well counter counts/ml/min using the calibration

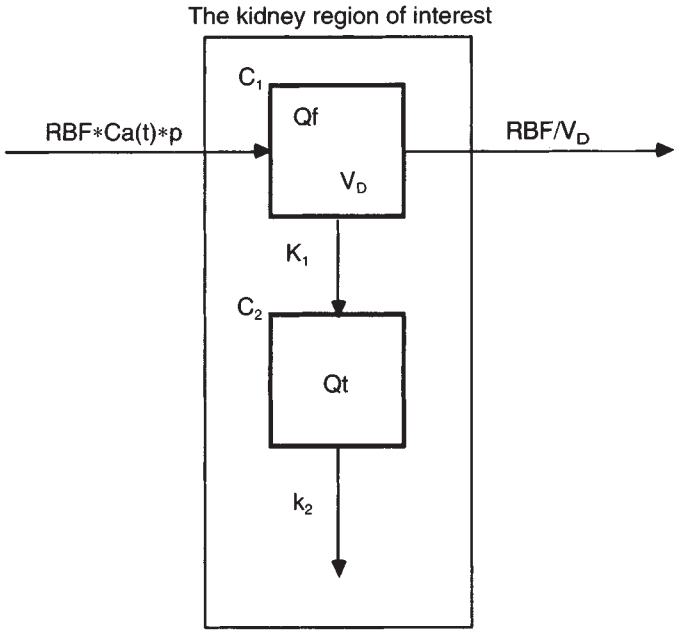

Fig. 1. *The two-compartment model for N-13 ammonia RBF quantification.* The rectangle indicates the kidney region of interest.

factor. All time-activity curves were corrected for dead time of the scanner [12].

Partial volume effects result in less than 100% recovery of tissue activity in structures measuring less than about twice the full-width half-maximum image resolution value [13]. These activity losses can be corrected if the recovery coefficient is known. We employed an approach developed in our laboratory for the calculation of the recovery coefficients in the animal studies [14]. This approach is based on cross-sectional profile fitting analysis. In brief, each circular ROI drawn over the renal cortex was divided in four subsectors. The estimates of activity thicknesses, together with four known subsector contour thicknesses, were used to derive four subsector recovery coefficients. These subsector recovery coefficients were then combined into one recovery coefficient for the renal cortical ROI. In the human studies estimates for the recovery coefficients were based on ultrasound measurements of the renal cortical thickness.

The true tissue activity concentration in the renal cortex was calculated as the observed radiotracer concentration divided by the recovery coefficient.

Patlak graphical analysis for the quantification of RBF

The Patlak approach is a graphical method for estimating the unidirectional blood-to-renal tissue transfer constant from renal time-activity uptake data. The approach assumes unidirectional transport and trapping of N-13 ammonia from blood into tissue. The total N-13 activity observed in a region of interest represents the sum of activities in two functional compartments: compartment 1 (C_1) contains the free N-13 ammonia in renal tissue and extravascular space, while compartment 2 (C_2) contains the tubular bound or trapped N-13 activity, as shown in Figure 1. The rate of N-13 change in compartment C_1, dQf(t)/dt, and the trapped N-13 in compartment C_2, dQt(t)/dt, in the kidney are expressed by the following equations:

$$\frac{dQf(t)}{dt} = -\frac{K_1 + RBF}{V_D} Qf(t) + RBF \cdot Ca(t) \cdot p \qquad \text{(eq. 1)}$$

and

$$\frac{dQt(t)}{dt} = \frac{K_1}{V_D} Qf(t) - k_2 Qt(t) \qquad \text{(eq. 2)}$$

where RBF is the renal blood flow in ml/min/g, Qf and Qt are the total N-13 activity (counts/ml/min) in compartments C_1 and C_2, respectively, K_1 the forward rate constant in ml/min/g from Qf to Qt, k_2 the tubular clearance constant in min^{-1} from Qt to the tubular lumen, V_D the distribution volume in ml/g of N-13 ammonia within the free space (0.8 ml/g [4]), Ca(t) the arterial activity of N-13 ammonia in counts/min/ml, p the specific gravity of blood (1.05 g/ml) and t the time in minutes. Thus, RCBF can be calculated by solving these differential equations describing the two-compartment model and by fitting to the measured renal tissue time-activity curves. This approach has been validated for RCBF ranging 1 to 6.5 ml/min/g against independent microsphere measurements [4].

For the graphical analysis approach the Patlak plot of the multiple-time renal tissue uptake is defined as the ratio of the total renal tissue concentration at the times of sampling to the plasma concentration (Ca) at the respective times (t) versus the ratio of the arterial plasma concentration-time integral to the plasma concentration (Ca), as described by equation 7 (listed below). This equation is derived in the following way: If k_2 is assumed to be 0 and equations 1 and 2 are integrated, then

$$Qf(t) = -\frac{K_1 + RBF}{V_D} \int_0^t Qf(t)dt + RBF \cdot p \int_0^t Ca(t)dt \qquad \text{(eq. 3)}$$

and

$$Qt(t) = \frac{K_1}{V_D} \int_0^t Qf(t)dt \qquad \text{(eq. 4)}$$

At time t after tracer injection, the N-13 activity concentration in renal tissue ROI [Qi(t)] equals the sum of the radioactivity of free N-13 ammonia in the freely diffusible pool Qf(t), the radioactivity of N-13 ammonia metabolites in the bound pool Qt(t) and the arterial concentration of the radiopharmaceutical (AB). This relationship is expressed by

$$Qi(t) = Qf(t) + Qt(t) + [V_V \cdot AB(t)] \qquad \text{(eq. 5)}$$

where V_V is the vascular volume and AB the arterial N-13 activity uncorrected for metabolite concentrations. Note the difference between Ca(t), defined as metabolite corrected N-13 activity and AB, defined as non-metabolite corrected N-13 activity.

Substituting Qf(t) and Qt(t) in equation 5 by equations 3 and 4, expressing the time integral of Qf(t) for that of Ca(t), and including the relationship from equation 1 that

$$Qf(t) = [RBF \cdot V_D/(K_1 + RBF)] \cdot Ca(t) \qquad \text{(eq. 6)}$$

at large t when $dQf(t)/dt \sim 0$ and assuming that p equals 1 g/ml and that AB(t) equals Ca(t) at $t \leq 90$ seconds, one can obtain a Patlak equation for calculation of RBF:

$$\frac{Qf(t)}{Ca(t)} = K_i \frac{\int_0^t Ca(\tau)d\tau}{Ca(t)} + \frac{RBF^2 \cdot V_D}{(RBF + K_1)^2} + V_V \quad \text{(eq. 7)}$$

where K_i is the slope of the straight portion of the Patlak plot and describes the rate of tracer delivery from arterial blood to the precursor (freely diffusible) pool times the fraction trapped in the bound pool. K_i can be expressed by

$$K_i = RBF \cdot K_1/(RBF + K_1) \quad \text{(eq. 8)}$$

or

$$K_i = RBF \cdot E_r \quad \text{(eq. 9)}$$

when including the retention fraction (E_r) for N-13 ammonia in the kidney

$$[E_r = 1 - 0.83 \times e^{(-1.353/RBF)}], \quad \text{(eq. 10)}$$

derived from dog kidney studies [4]. RBF can then be calculated using equations 9 and 10, by first estimating the slope K_i of the straight portion of the graph, with Qf(t)/Ca(t) as the vertical y-axis and $\int_0^t Ca(\tau)d\tau/Ca(t)$ as the horizontal x-axis [15].

N-13 ammonia is secreted into the renal tubules. Therefore, N-13 activity will proceed into the tubular lumen and leave the region of interest assigned to the renal cortex. Activity concentrations will decline, and the assumption of a unidirectional transport or k_2 to be zero is no longer valid. Hence, the assumption of a unidirectional transport model for N-13 ammonia is valid only early after tracer accumulation in the renal cortex. Proper selection of the time period for data analysis based on the time-activity curves is therefore critical. Consequently, only the kinetic data recorded from 40 to 90 seconds after tracer injection were used in the Patlak approach. In addition, effects of including earlier or later recorded kinetic data on the Patlak estimates of RCBF were evaluated.

If the assumptions are valid, then the fit to the kinetic data will be linear. The slope represents K_i and the y-intercept will depend on the distribution volume (V_D), on renal blood flow (RBF), on the forward rate constant from Qf to Qt (K_1) and on the vascular volume (V_V). Again, the regression line will be linear only if k_2 is indeed 0 for the time of measurement.

The O-15 water technique to quantify RBF

The theory for the measurement of blood flow using the inert freely diffusible O-15 water was described for the kidney by Inaba et al [7], and for myocardium by Bergmann et al [16] and Iida et al [17]. The general principles have been proposed by Kety [18]. Kuten et al observed a high correlation of RBF estimates by O-15 water and estimates by independent microsphere RBF measurements [19]. Figure 2 illustrates the one compartment model used for estimating RBF with O-15 water. The following differential equation describes the rate of change of O-15 water within the kidney:

$$\frac{dCt}{dt} = \frac{RBF}{V} Ca - \frac{RBF}{\rho V} Ct \quad \text{(eq. 11)}$$

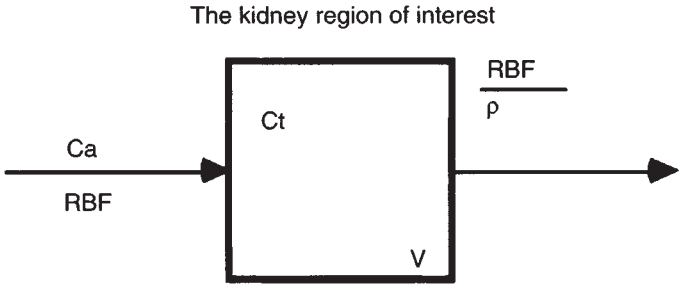

Fig. 2. *The one-compartment model for O-15 water RBF quantification.* The rectangle indicates the kidney region of interest.

where Ct is the O-15 water activity in the ROI in counts/pixel/min and V is the distribution volume of water in renal tissue within the ROI (ml). The constant ρ is determined by the tissue/blood partition coefficient (ml/g), the specific gravity of the kidney and the extraction fraction of O-15 water in the kidney. Solving equation 11 for Ct yields

$$Ct = \frac{RBF}{V} \int_0^t e^{-\frac{RBF}{\rho V}(t-\tau)} Ca(\tau)d\tau \quad \text{(eq. 12)}$$

Simplifying equation 12 by expressing

$$RBF/\rho V = k \quad \text{(eq. 13)}$$

one derives

$$Ct = Ca(t) \otimes \rho k e^{-kt} \quad \text{(eq. 14)}$$

where the asterisk ($\otimes$) indicates the mathematical operation of convolution. Integrating equation 14 for the scan time duration t_i to t_{i+1} yields

$$\int_{ti}^{ti+1} Ctdt = \int_{ti}^{ti+1} Ca(t) \otimes \rho k e^{-kt} dt \quad \text{(eq. 15)}$$

$\int_{t1}^{ti+1} Ctdt$ is measured by PET for $t = t_i$ to t_{i+1} for $i = 1 \ldots 12$ and $\int_{ti}^{ti+1} Ca(t) \otimes \rho k e^{-kt}$ is calculated using the one-compartment model and the arterial input function for a given ρ and renal blood flow. RCBF was then estimated by using equation 15 to fit the measured renal time-activity curves.

Several methods are available to correct for intravascular activity within the tissue ROI before finally estimating RCBF. One employs blood pool images obtained with O-15 or C-11 carbon monoxide and subtraction of these images from the O-15 water images. A second approach adds a third parameter to the one-compartment model to estimate the blood pool. In the present study, a third parameter for calculation of the blood pool activity [vascular blood pool in renal tissue (RBV) observed in the analyzed ROI] was added to the O-15 water model to correct for intravascular activity within tissue ROI's [20, 21]. This approach was chosen in this study because direct measurements of renal intravascular volume with O-15 carbon monoxide renal blood pool imaging would have required an additional imaging procedure, with its inherent compounding of errors. Incorporating RBV in equation 15 yields

$$\int_{ti}^{ti+1} Ctdt = \int_{ti}^{ti+1} Ca(t) \otimes \rho k e^{-kt} dt + RBV \cdot Ca(t) \quad \text{(eq. 16)}$$

The input function was derived from peripheral arterial blood sampling. Its inherent problem is the time delay between the aortic and the peripheral (such as, brachial) peak activity. To minimize errors potentially introduced by the time delays between the input function and the tissue response, the peak activity of the arterial input function was adjusted to the time of the aortic peak activity. The latter was determined from a circular ROI (size 6 ± 3 pixel) assigned to the abdominal aorta.

The RCBF value for one kidney was calculated as the average value for all analyzed ROI per kidney.

Parametric imaging

Parametric images of RCBF using N-13 ammonia and Patlak graphical analysis were generated by applying equations 7 and 9 to each pixel.

Statistical analysis

All results are expressed as mean ± standard deviation (SD). Linear least-squares regression was performed to correlate RCBF calculated with the two-compartment model and Patlak graphical analysis for N-13 ammonia measurements in humans and animals. For evaluation of mean differences in the reproducibility for N-13 ammonia and O-15 water RCBF studies as well as differences between N-13 ammonia and O-15 water RCBF measurements, the paired *t*-test was used. A P value < 0.05 was considered significant.

Results

N-13 ammonia renal imaging and Patlak graphical analysis

N-13 ammonia yielded high quality cross-sectional images of the kidneys with PET imaging. The image quality was preserved even when RCBF was markedly altered as was the case in the pig experiments (Fig. 3). As shown in Figure 4, the Patlak plots of the time-activity curves for all analyzed ROI were consistently linear for the selected sampling times. If earlier (such as 20 to 30 seconds post-injection) recorded renal tissue points were included for the Patlak graphical analysis, the calculated RCBF values did not correlate as well with model fitting results, because that part of the data is not expected to be linear. In addition, if more (such as >90 seconds post-injection) renal tissue points were included, the curve of the Patlak plot became nonlinear, indicating that the definition (such as the tubular clearance k_2 is negligible) for Patlak graphical analysis may no longer be satisfied. For k_2 ranging from 0 min^{-1} to 0.2 min^{-1} after 110 seconds post-injection the change of the RCBF estimates was less than 5%. It was similar at both high and low RCBF values.

Comparison of Patlak graphical analysis and the two-compartment model

Animal studies. Estimates of RCBF derived by the Patlak graphical analysis correlated linearly with estimates obtained by the two-compartment model fitting ($y = -0.05 + 1.01x$, $r = 0.99$) as illustrated in Figure 5. RCBF ranged 0.18 to 6.35 ml/min/g.

Human studies. As shown in Figure 6, there is a linear correlation between estimates of RCBF by Patlak graphical analysis and those by the two-compartment model in normal human volunteers. The slope of the regression line and the correlation coefficient are slightly less than in the pig studies ($y = 0.57 + 0.88x$, $r = 0.93$). One reproducibility study with N-13 ammonia was not performed because the isotope production failed. Therefore, the results reported above refer to 29 N-13 ammonia dynamic PET studies. Estimates of normal RCBF by the N-13 ammonia PET approach averaged 4.64 ± 0.48 ml/min/g for Patlak graphical analysis and 4.61 ± 0.51 ml/min/g for model fitting.

O-15 water studies

O-15 water dynamic PET renal images compared to N-13 ammonia renal PET images have lower image quality, such as lower kidney to background ratio. However, both kidneys are depicted clearly in normal human volunteers (Fig. 7). Estimates of normal RCBF by the O-15 water approach averaged 4.70 ± 0.28 ml/min/g. The added third parameter to the one-compartment model for O-15 water renal studies produced estimates of the blood pool present in the arterial bed in the analyzed cortical tissue ROI. The observed value of this parameter was 0.16 ± 0.11 ml/g.

Comparison of RCBF estimates derived from N-13 ammonia and O-15 water studies

As shown in Figure 8, the estimates of RCBF for both radiopharmaceuticals in human normals were linearly correlated. The differences between the N-13 ammonia and the O-15 water RCBF estimates were statistically insignificant. A P value of 0.48 for Patlak graphical analysis RCBF estimates and a P value of 0.23 for the two-compartment model fitting RCBF estimates compared to O-15 water RCBF estimates were observed.

Reproducibility of RCBF measurements

Heart rate and blood pressure remained stable in all subjects during the PET measurements. Repeat measurements of RCBF with N-13 ammonia and dynamic PET in nine volunteers revealed for Patlak graphical analysis individual interstudy differences of 0.31 ± 0.18 ml/min/g or 6.6% ± 3.7% ($P = 0.91$) and for model fitting 0.22 ± 0.15 ml/min/g or 5.0% ± 3.4% ($P = 0.62$). Absolute individual interstudy differences for O-15 water measurements in five volunteers were 0.11 ± 0.07 ml/min/g or 2.2% ± 1.3% ($P = 0.12$). The interstudy differences of the RCBF estimates within each individual approach were insignificant.

N-13 ammonia metabolites

The results of N-13 ammonia metabolite measurements are shown in Table 1. The mean amount of N-13 labeled ammonia metabolites as fraction of the total N-13 activity at two minutes post injection was 7% ± 5% for human normals while in pigs it was 10.5% ± 2%.

Thickness of the renal cortex

Circumferential profile fitting analysis revealed the following average estimates for renal cortical thickness in the pig experiments: 11.8 ± 0.7 mm for normal kidneys, 13.9 ± 1.2 mm for acute tubular necrosis, 14.0 ± 0.5 mm for acute rejection, 13.5 ± 1.4 mm for renal hypertrophy and 11.6 ± 0.5 mm for cyclosporine toxicity. These results indicate an increasing renal

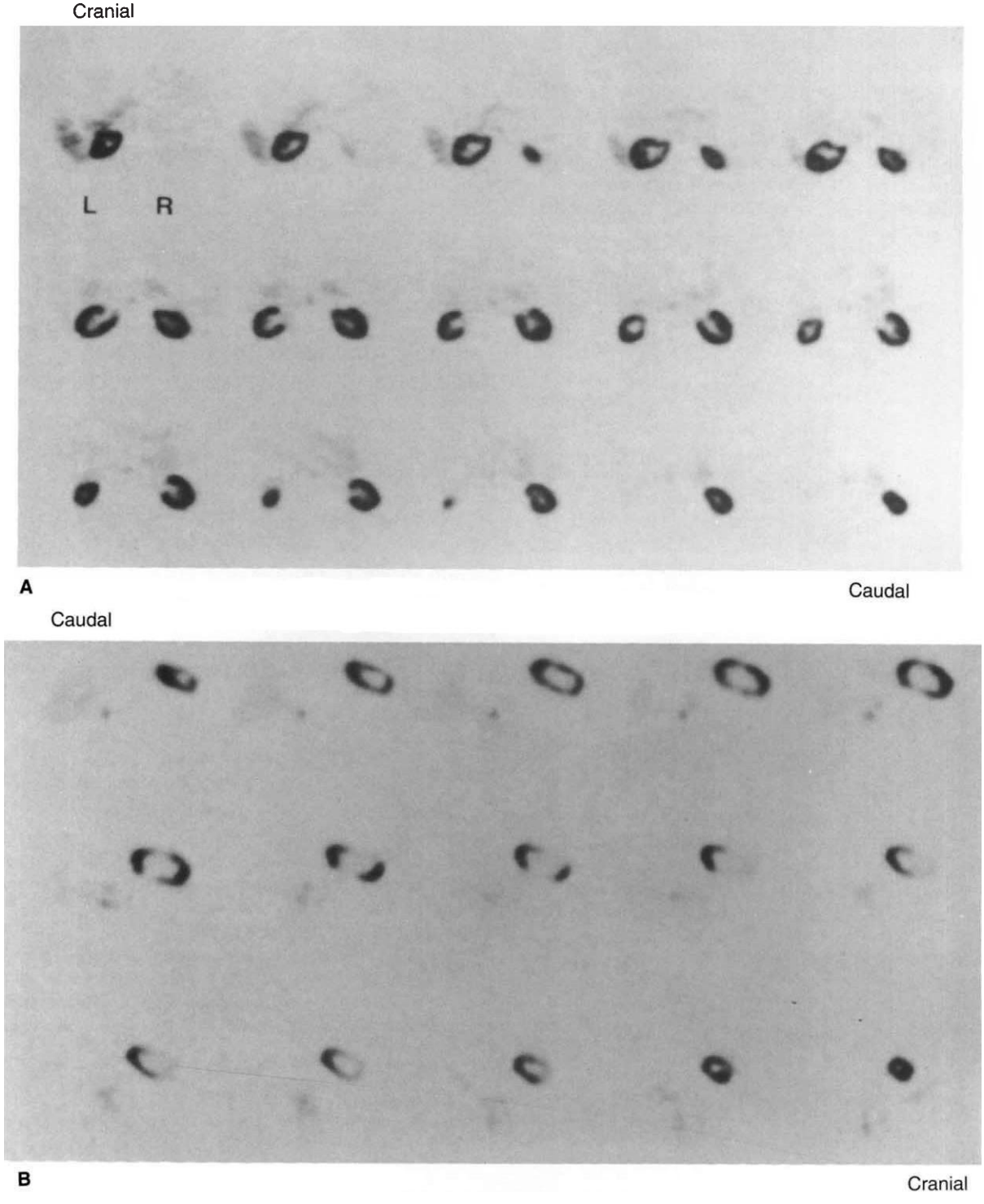

Fig. 3. *N-13 ammonia cross sectional images of the kidneys.* **(a)** Summed dynamic PET images [0 to 2 min post-injection (p.i.)] of normal kidneys in a healthy human volunteer (p04092). N-13 ammonia indicates normal RCBF, left: 4.76 ml/min/g, right: 4.71 ml/min/g. **(b)** Summed dynamic PET images (0 to 2 min p.i.) of a transplant kidney in acute rejection in a pig (A00577). N-13 ammonia indicates markedly reduced RCBF: 0.55 ml/min/g, as well as flow defects within the kidney. **(c)** Summed dynamic PET images (0 to 2 min p.i.) of a transplant kidney in acute tubular necrosis in a pig (A00534). N-13 ammonia indicates markedly reduced RCBF: 0.88 ml/min/g.

cortical thickness caused by renal parenchyma swelling induced by ischemia in acute tubular necrosis and acute rejection. This increase was only transient in acute tubular necrosis but persistent in acute rejection, at least for the time period of the study. The latter trend, resulting from cellular hypertrophy, was also observed for renal hypertrophy following unilateral

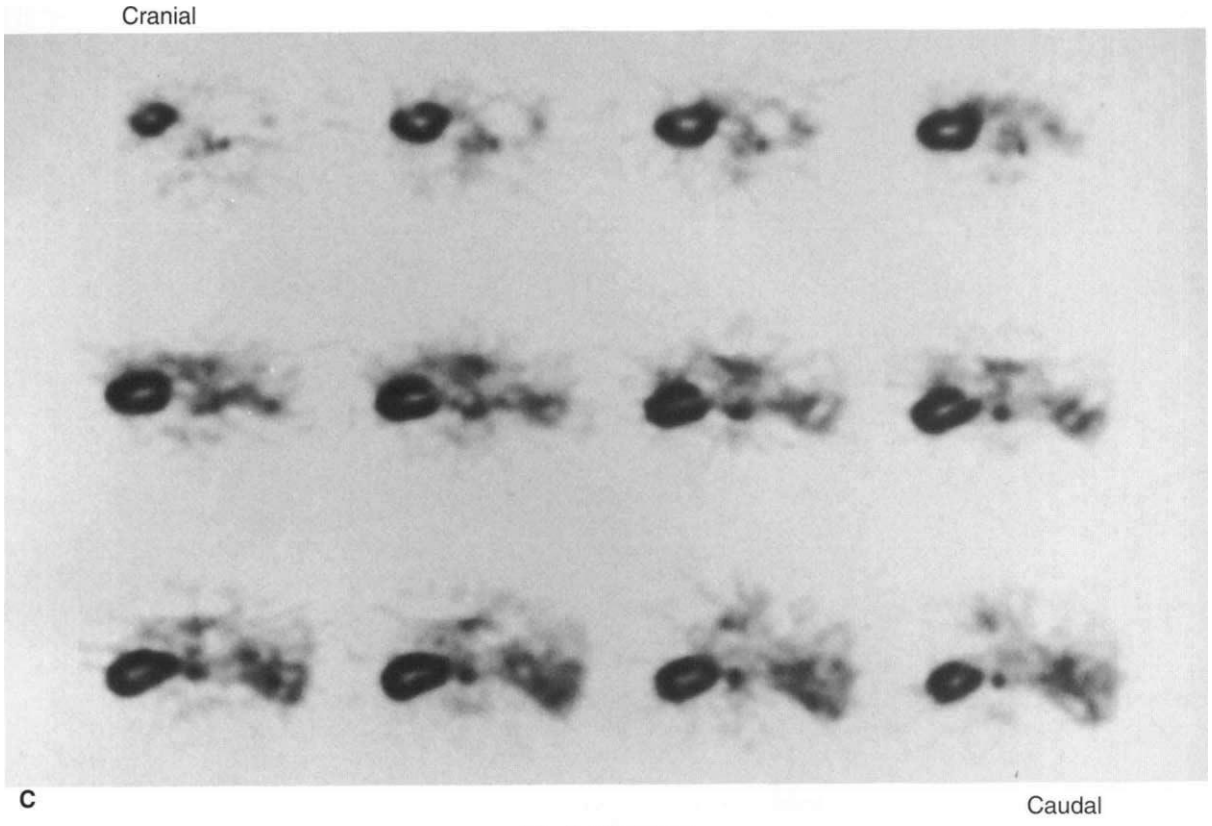

Fig. 3. *Continued.*

nephrectomy. Cyclosporine toxicity did not affect renal cortex thickness. For the normal human kidneys a renal cortical thickness of 12.0 ± 0.7 mm was calculated. It was similar to ultrasound estimates, 11.5 ± 1.0 mm.

Parametric imaging

As shown in Figure 9, parametric images of RCBF contain less noise and therefore an improved kidney to background ratio as compared to dynamic renal images.

Computation time

The computation time for the Patlak approach to estimate RCBF in a 15 plane dynamic study is two minutes. This is ~50% faster as compared to approximately four to five minutes for the model fitting method.

Discussion

The results of this study indicate that the kinetics of N-13 ammonia in the kidney following intravenous injection satisfy the requirements of Patlak graphical analysis. Therefore, Patlak graphical analysis can be applied to quantify RCBF. Moreover, Patlak graphical analysis produces RCBF estimates comparable to those obtained with the two-compartment model method for N-13 ammonia. Further, the excellent agreement of the N-13 ammonia estimates of RCBF with those by the metabolically inert and less flow dependent O-15 water method supports the validity of the N-13 ammonia technique in humans, which, as demonstrated by repeat measurements, is highly reproducible.

Comparison of RCBF estimates derived from Patlak graphical analysis and the two-compartment model for N-13 ammonia

The slightly better correlation between Patlak graphical analysis and model fitting in the pig experiments (Fig. 5) as compared to the correlation in the human studies (Fig. 6) may have been due to the narrow range of RCBF's in humans and better count statistics in the animal experiments.

Quantification of RCBF with dynamic PET and N-13 ammonia or O-15 water and its limitations in the present study

The PET technique for measurements of RBF has been successfully employed by several groups [4, 7, 22, 23] as well as in the present study. For renal PET imaging in humans, only O-15 water and N-13 ammonia have been used. We prefer N-13 ammonia over O-15 water for RBF imaging because of the better count statistics and therefore better image quality. An additional advantage is the suitability of N-13 ammonia for generating parametric images of RCBF based on Patlak graphical analysis. Studies from other laboratories using the external detector or PET techniques have reported the feasibility of rubidium-82 as indicator of RBF in dogs. RBF ranged 0.2 to 5.5 ml/min/g [22–24]. The validity of rubidium-82 as RBF agent in humans has not yet been confirmed. Despite the present study one group recently employed O-15 water for dynamic PET

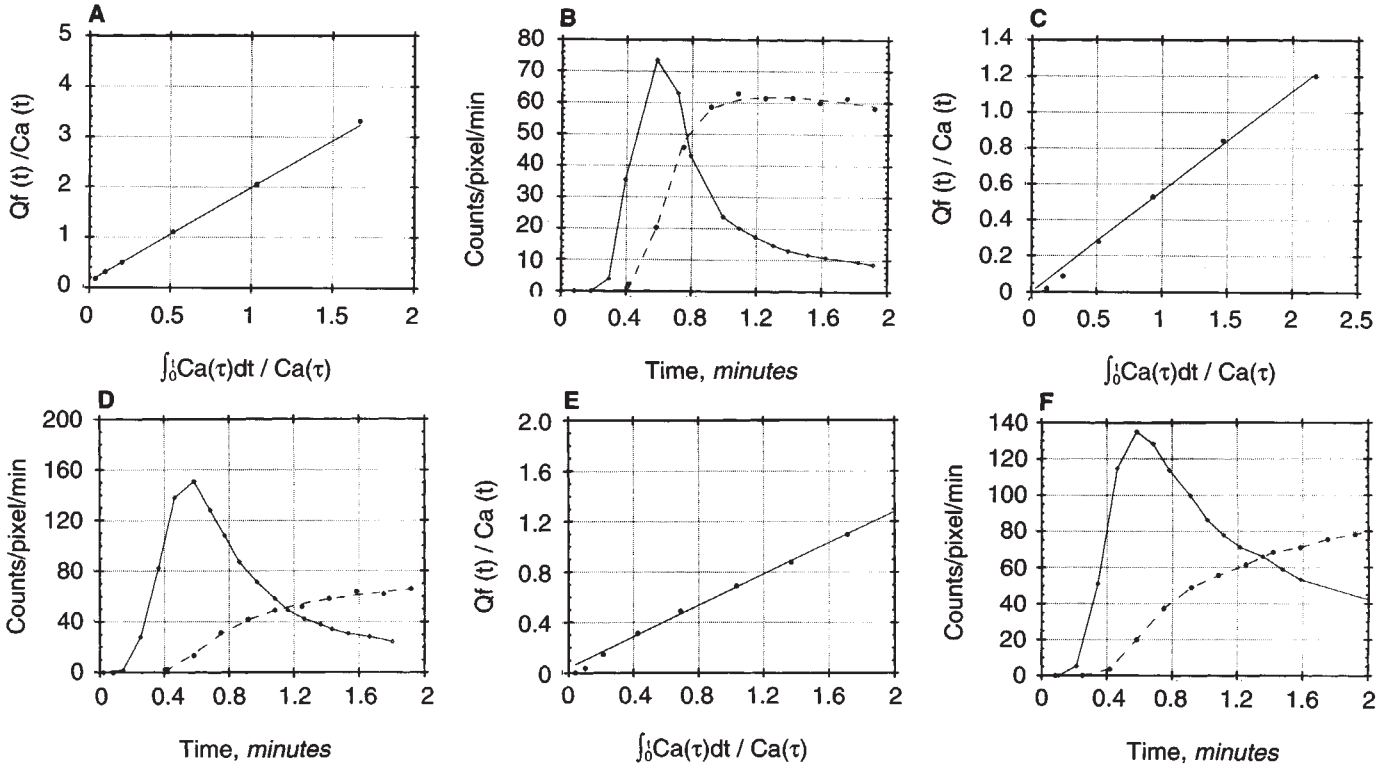

Fig. 4. *The Patlak graph.* **(A)** Plot of a Patlak graph from a study in a healthy human volunteer (P04092). Filled circles are the data points, while the straight line is a linear fit to the data from 40 to 90 sec p.i., RCBF: 4.65 ml/min/g. **(B)** Corresponding plot of the fit (0 to 2 min p.i.) of the two-compartment model to the renal time-activity curve (dashed line), RCBF: 4.72 ml/min/g. Solid line represents the time-activity curve for the arterial input function. **(C)** Plot of a Patlak graph from a study in a pig (A00577) for evaluation of acute rejection. Data from 40 to 90 seconds p.i. are linearly fitted. RCBF is markedly altered: 0.51 ml/min/g, compared to normal RCBF in pigs: 3.20 ml/min/g. **(D)** Corresponding plot of the fit (0 to 2 min p.i.) of the two-compartment model to the renal time-activity curve (dashed line). Solid line represents time-activity curve for the arterial input function. RCBF: 0.55 ml/min/g. **(E)** Plot of a Patlak graph from a study in a pig (A00534) for evaluation of acute tubular necrosis. Data from 40 to 90 sec p.i. are linearly fitted. RCBF is markedly altered: 0.85 ml/min/g. **(F)** Corresponding plot of the fit (0 to 2 min p.i.) of the two-compartment model to the renal time-activity curve (dashed line). Solid line represents time-activity curve for the arterial input function. RCBF: 0.87 ml/min/g.

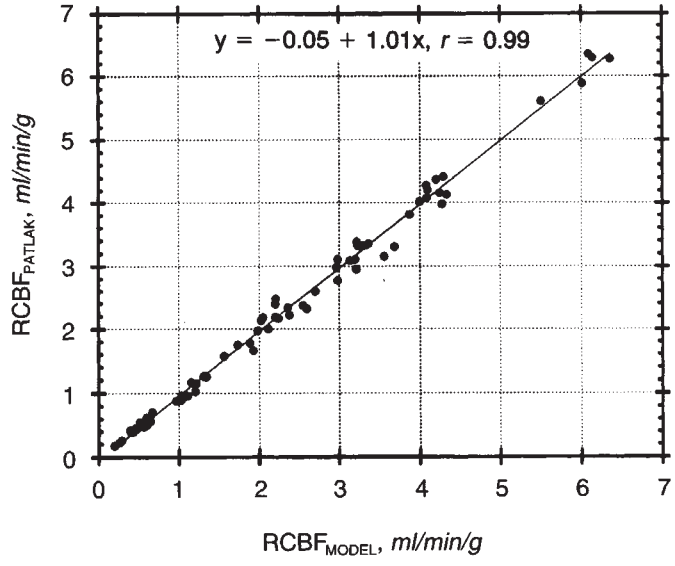

Fig. 5. *Correlation of Patlak graphical analysis and the two-compartment model for RCBF quantification in the pig studies* (N = *10 pigs*, N = *59 studies*, N = *71 kidneys*). y = −0.05 + 1.01x, *r* = 0.99.

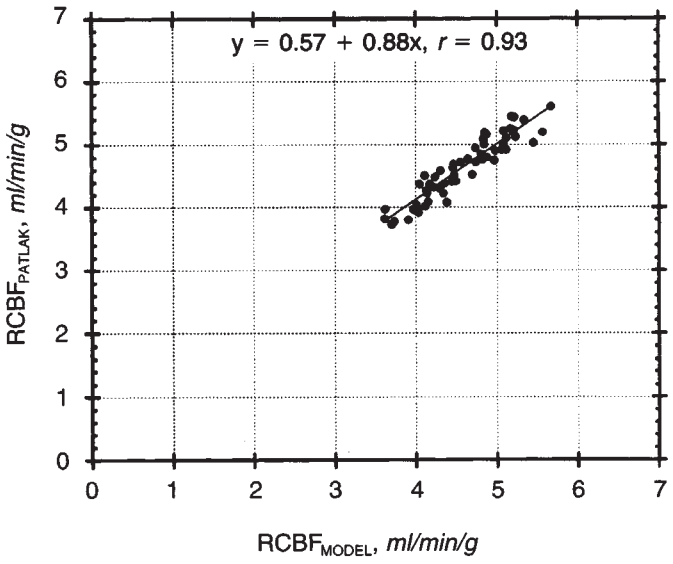

Fig. 6. *Correlation of Patlak graphical analysis and the two-compartment model for RCBF quantification in 20 normal human volunteers* (N = *29 studies*, N = *58 kidneys*). y = 0.57 + 0.88x, *r* = 0.94.

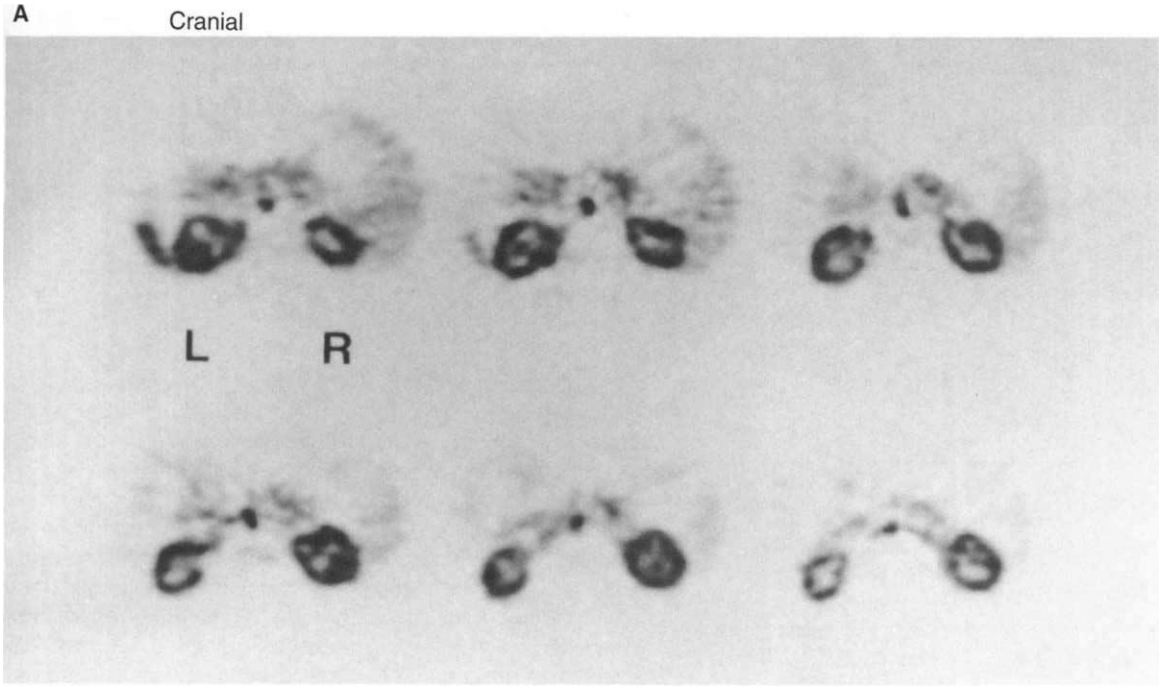

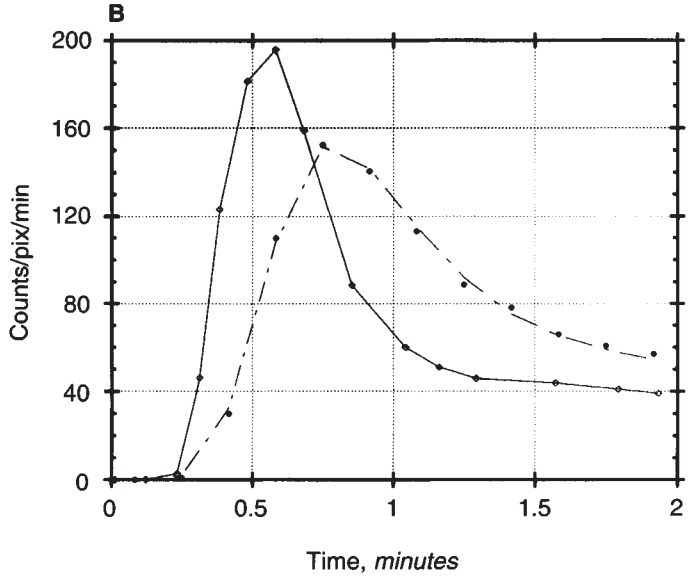

Fig. 7. *O-15 water cross-sectional images of the kidneys and a plot of an one-compartment model fitting graph.* **(A)** Summed dynamic PET images of the kidneys of a dynamic O-15 water study in a healthy human volunteer (P04092). **(B)** Plot of the fit (dashed line, 0-2 min p.i.) of the one-compartment model to the renal time-activity curve. Solid line represents the time-activity curve for the arterial input function, RCBF: 4.85 ml/min/g.

measurements of RBF in eight human subjects [7]. The advantage of O-15 water as RBF agent is that it is metabolically inert and completely extracted in renal tissue. In contrast, N-13 ammonia is not metabolically inert and its retention fraction declines as RBF increases above the normal range [4]. For the latter reason it is necessary to include the relationship between RBF and retention fraction. This relationship is mathematically expressed by equations 9 and 10. Both equations are incorporated in the Patlak and the two-compartment model fitting approach. Its limitation is the derivation from animal studies because microsphere studies cannot be performed in humans. However, the good agreement between RCBF estimates obtained by both, the O-15 water and N-13 ammonia PET approach provides evidence of the validity of N-13 ammonia as RBF agent in humans. For the clinical applications of N-13 ammonia, one is most likely referred to decreased or normal RBF rather than the evaluation of the hyperemic RBF response. For both conditions, N-13 ammonia provided high quality images and comparable RCBF estimates even if RCBF was markedly altered.

A potential disadvantage of the O-15 water technique is the need for blood volume correction for each individual RBF study. Inaba et al [7] utilized O-15 carbon monoxide PET imaging for blood volume correction. The fraction of radioactivity due to O-15 water in the vascular spaces was removed by subtracting O-15 carbon monoxide images from corresponding

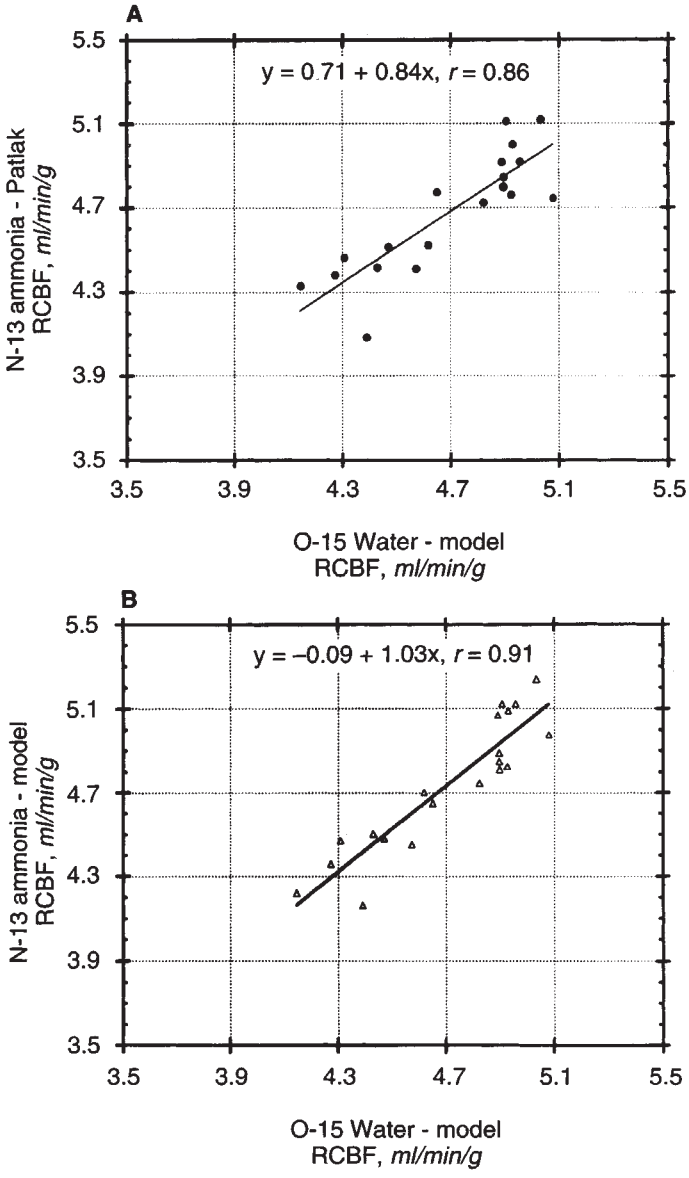

Fig. 8. *Correlation of estimates of RCBF by* (**A**) Patlak graphical analysis (y = 0.71 + 0.84x, r = 0.86) and (**B**) the two-compartment model for N-13 ammonia dynamic PET (y = −0.09 + 1.03x, r = 0.91) compared to estimates of the one-compartment model fitting for O-15 water.

O-15 water emission images. Inaccuracies in the subtraction process may cause errors in the estimation of RBF [25]. For the present study, a third parameter was added to the one-compartment model for O-15 water in order to correct for blood volume effects. Including the blood volume term in the fitting procedure was found by others to be superior to the subtraction method, both in terms of accuracy and precision [21]. The correction approach may also have contributed to the good agreement between N-13 ammonia and O-15 water RCBF estimates observed in this study.

N-13 ammonia metabolites

Accurate quantification of RCBF based on N-13 ammonia dynamic PET studies requires appropriate correction for the contamination of the arterial input function by N-13 labeled ammonia metabolites. The observed percentage of non-ammonia metabolites of 7% ± 5% in our normal humans is comparable to the reported percentage (6% ± 3%) obtained from venous whole blood sampling for the respective time period in human normals [26]. While serial arterial blood sampling for measurements of N-13 labeled ammonia metabolites adds complexity to human clinical RBF studies, alternative methods to minimize invasiveness and inaccuracy are of potential interest. The independent observation of comparable N-13 labeled ammonia metabolite blood concentrations by two study groups suggests two methods. The interpolation of N-13 labeled metabolite concentrations measured in venous blood samples represents one method. Routine computational incorporation of reported metabolite concentrations may be an alternative method. Use of an uncorrected arterial input function may cause some underestimation of RBF. Based on the data in this study, this underestimation would amount to 5.1% ± 0.9%, which if consistent, may also be acceptable in the clinical setting and render the approach rather noninvasive. For animal studies, observations from the same group [26] as well as in this study indicate that there are species differences in the blood concentrations of N-13 labeled ammonia metabolites within the two minutes post injection time period, such as 19% ± 16% for dogs and 10.5% ± 2% for pigs. These observations suggest the need for metabolite correction when N-13 ammonia is utilized for RBF studies in animals.

Table 1. The percentage of true N-13 ammonia over a time interval of two minutes as determined from serial arterial blood sampling after peripheral intravenous injection (p.i.) of N-13 ammonia

	Percentage of true N-13 ammonia (mean ± SD)	
Time post-p.i. *min*	Humans	Pigs
0.66	99.24 ± 0.66	99.28 ± 0.31
1.33	97.75 ± 1.73	96.78 ± 1.14
2.00	93.07 ± 5.22	89.52 ± 1.82

Minimization of invasiveness to obtain the input function

Determination of the arterial input function from serial blood samples, as performed in this study, adds complexity to routine clinical procedures. However, alternative methods include sampling from the arterial part of an arterio-venous shunt or dynamic PET measurements of the abdominal aortic activity for the non-invasive determination of the arterial input function [27].

Recovery coefficients for renal cortex

Corrections for partial-volume effects (such as renal cortex recovery coefficient) are relatively straightforward in the normal human kidney where cortex and medulla are identifiable sonographically. However, in human kidney transplants, anatomical measurements based on ultrasound do not provide appropriate measures of the renal cortex thickness. In such conditions, use of cross-sectional profile fitting analysis or constant recovery coefficients may be preferable. The results

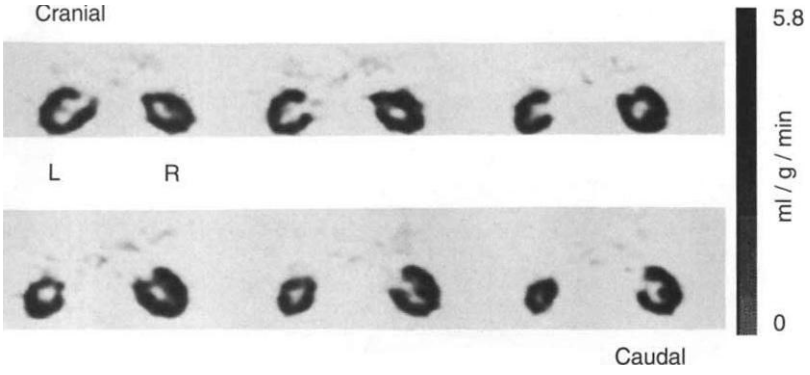

Fig. 9. *Parametric cross-sectional image of N-13 ammonia indicated RCBF, generated from a study in a healthy human volunteer (P04092).*

Table 2. Comparison between normal RCBF values produced by PET and the Xenon-133 washout method

Method	Approach	RCBF *ml/min/g*
PET N-13 ammonia	Patlak graphical analysis	4.64 ± 0.48
PET N-13 ammonia	Two-compartment model	4.61 ± 0.51
PET O-15 water	One-compartment model	4.70 ± 0.28
Xenon-133 washout		4.10 ± 0.90 [28]
Xenon-133 washout		5.38 ± 0.86 [29]

based on pig experiments indicate the need for such a compromise for non-physiological conditions like acute tubular necrosis, acute rejection or renal hypertrophy, when accurate anatomical measurements for the object size are not available. The recovery coefficient can differ significantly (for example, normal cortex value of ~0.65 to ~0.75 compared to acute tubular necrosis value of ~0.75 to ~0.85). Since this variability affects Patlak graphical analysis and model fitting results in the same way, this is not a limitation specific to the Patlak method.

Parametric images of N-13 ammonia indicated RCBF

Parametric PET imaging of RCBF is an advantageous approach particularly for the clinical setting. It provides dynamically acquired geographic information about RCBF compressed in a single renal PET image. In addition, the unspecific background noise is suppressed rendering improved image quality compared to dynamic renal PET images.

RCBF in human normals measured by dynamic PET compared to the Xenon-133 washout method

In the renal cortex blood flow averages 4 to 6 ml/min/g as indicated from measurements in different animal species and human studies [28]. The RCBF values measured with PET in human normals in this study are comparable to those by the Xenon-133 washout method [29, 30] listed in Table 2. The slightly higher RCBF values reported by Ladefoged and Pederson [30] may be explained by the small age range of the volunteers and possible differences in the sodium balance.

Clinical RCBF studies based on dynamic PET

PET offers assessment of RBF without urine collection, as required in standard clearance techniques. Therefore, PET is applicable to the oliguric state. RBF can be measured noninvasively within a reasonable time as for example 30 minutes. RBF analysis can be performed on data acquired dynamically over three to five minutes. Repeat measurements can be performed within a short time period. Information about compartmental RBF is provided, not obtained from gamma camera renal studies or clearance methods. Finally, the radiotracer can be administered intravenously.

Conclusion

Patlak graphical analysis applied to N-13 ammonia dynamic PET for quantifying RCBF *in vivo* in humans is an accurate, reproducible and computationally fast method for investigative and clinical applications. N-13 ammonia is a valid RCBF indicator in humans compared to the O-15 water technique. Quantification of RCBF with dynamic PET is highly reproducible. Parametric imaging of N-13 ammonia indicated RCBF is an advanced imaging approach for the clinical setting.

Acknowledgments

Operated for the US Department of Energy by the University of California under contract #DE-FC03-87ER60615. This work was supported in part by the Director of the Office of Energy Research, Office of Health and Environmental Research, Washington, DC, by Research Grants #HL 29845 and #HL 33177, National Institutes of Health, Bethesda, Maryland and by an Investigative Group Award by the Greater Los Angeles Affiliate of the American Heart Association, Los Angeles, California. The authors thank their PET technologists Ronald Sumida, Lawrence Pang, Judy Edwards, Francine Aquilar, Der-Jenn Liu and Mark Hulgan for carrying out the PET scanning, Anh Nguyen for assistance in measuring the ammonia metabolite concentrations, and the UCLA Medical Cyclotron staff for the production of the radiopharmaceuticals.

Reprint requests to Henrich R. Schelbert, M.D., Division of Nuclear Medicine & Biophysics, UCLA School of Medicine, 10833 Le Conte Avenue, Los Angeles, California 90024-6948, USA.

References

1. Carriere S: Factors affecting renal cortical blood flow. *Can J Physiol Pharmacol* 53:1–20, 1975
2. Aukland K: Methods for measuring renal blood flow: Total flow and regional distribution. *Annu Rev Physiol* 42:543–555, 1980
3. Dworkin LD, Brenner BM: The renal circulations, in *The Kidney* (4th ed), edited by Brenner BM, Rector FC, Philadelphia, WB Saunders, 1991, pp. 164–204
4. Chen BC, Germano G, Huang SC, Hawkins RA, Hansen HW, Robert MJ, Buxton DB, Schelbert HR, Kurtz I, Phelps ME: A new noninvasive quantification of renal blood flow with N-13 ammonia, dynamic positron emission tomography and a two-compartment model. *J Am Soc Nephrol* 3:1295–1306, 1992

5. PATLAK CS, BLASBERG RG, FENSTERMACHER JD: Graphical evaluation of blood-to-brain transfer constants from multiple-time uptake data. *J Cereb Blood Flow Metab* 3:1–7, 1983
6. PATLAK CS, BLASBERG RG: Graphical evaluation of blood-to-brain transfer constants from multiple-time uptake data. Generalizations. *J Cereb Blood Flow Metab* 5:584–590, 1985
7. INABA T, YAMASHITA M, KAWASE Y, NAKAHASHI H, WATANABE H: Quantitative measurement of renal plasma flow by positron emission tomography with oxygen-15 water. *Tohoku J Exp Med* 159:283–289, 1989
8. YANAGA K, MAKOWKA L, SHIMADA M, LEBEAU G, KAHN D, MIELES LA, SHER L, CHAPCHAP P, PODESTA LG, STARZL TE: Improved method of porcine renal allografting for transplantation research. *J Invest Surg* 4:231–236, 1991
9. SCHELBERT HR, PHELPS ME, HUANG SC, MCDONALD NS, HANSEN H, SELIN C, KUHL DE: N-13 ammonia as an indicator of myocardial blood flow. *Circulation* 63:1259–1272, 1981
10. HUANG SC, CARSON RE, HOFFMAN EJ, CARSON J, MACDONALD N, BARRIO JR, PHELPS ME: Quantitative measurement of local cerebral blood flow in humans by positron computed tomography and ^{15}O-water. *J Cereb Blood Flow Metab* 3:141–153, 1983
11. KRIVOKAPICH J, BARRIO JR, PHELPS ME, WATANABE CR, KEEN RE, PADGETT HC, DOUGLAS E, SCHINE KI: Kinetic characterization of $^{13}NH_3$ and [^{13}N] glutamine metabolism in rabbit heart. *Am J Physiol* 246:H267–H273, 1984
12. GERMANO G, HOFFMAN EJ: An investigation of count rate capability and dead time for a high resolution PET system. (abstract) *J Nucl Med* 28:A607, 1987
13. HOFFMAN EJ, HUANG SC, PHELPS ME: Quantitation in positron emission tomography. I. Effect of object size. *J Comp Assist Tomogr* 3:299–308, 1979
14. KUHLE WG, PORENTA G, HUANG SC, BUXTON DB, GAMBHIR SS, HANSEN H, PHELPS ME, SCHELBERT HR: Quantification of regional myocardial blood flow using ^{13}N-ammonia and reoriented dynamic positron emission tomographic imaging. *Circulation* 86: 1004–1017, 1992
15. CHOI Y, HUANG SC, HAWKINS RA, KUHLE WG, DAHLBOM M, HOH CK, CZERNIN J, PHELPS ME, SCHELBERT HR: A simplified method for quantification of myocardial blood flow using N-13 ammonia and dynamic PET. *J Nucl Med* 34:488–497, 1993
16. BERGMANN SR, FOX KAA, RAND AL, MCELVANY KD, WELCH MJ, MARKHAM J, SOBEL BE: Quantification of regional myocardial blood flow *in vivo* with $H_2{}^{15}O$. *Circulation* 70:724–733, 1984
17. IIDA H, KANNO I, TAKAHASHI A, MIURA S, MURAKAMI M, TAKAHASHI K, ONO Y, SHISHIDO F, INUGAMI A, TOMURA N, HIGANO S, FUJITA H, SASAKI H, NAKAMICHI H, MIZUSAWA S, KONDO Y, UEMURA K: Measurement of absolute myocardial blood flow with $H_2{}^{15}O$ and dynamic positron emission tomography. Strategy for quantification in relation to the partial-volume effect. *Circulation* 78:104–115, 1988
18. KETY S: The theory and applications of the exchange of inert gas at the lungs and tissues. *Pharmacol Rev* 3:1–41, 1951
19. KUTEN A, ROVAL HD, GRIFFETH LK, MINTUM MA, PEREZ CA, WASSERMAN TH, TER-POGOSSIAN MM: Positron emission tomography in the study of acute radiation effects on renal blood flow in dogs. *Int Urol Nephrol* 24:527–529, 1992
20. HAWKINS RA, PHELPS ME, HUANG SC: Effects of temporal sampling, glucose metabolic rates, and disruptions of the blood-brain barrier on the FDG model with and without a vascular compartment: Studies in human brain tumors with PET. *J Cereb Blood Flow Metab* 6:170–183, 1986
21. LAMMERTSMA AA, DE SILVA R, ARAUJO LI, JONES T: Measurement of regional myocardial blood flow using $C^{15}O_2$ and positron emission tomography: Comparison of tracer models. *Clin Phys Physiol Meas* 13:1–20, 1992
22. TAMAKI N, RABITO CA, ALPERT NM, YASUDA T, CORREIA JA, BARLAI-KOVACH M, KANKE M, DRAGOTAKES SC, STRAUSS HW: Serial analysis of renal blood flow by positron emission tomography with rubidium-82. *Am J Physiol* 251:H1024–H1030, 1986
23. TAMAKI N, ALPERT NM, RABITO CA, BARLAI-KOVACH M, CORREIA JA, STRAUSS HW: The effect of captopril on renal blood flow in renal artery stenosis assessed by positron tomography with rubidium-82. *Hypertension* 11:217–222, 1988
24. MULLANI NA, EKAS RD, MARANI S, KIM EE, GOULD KL: Feasibility of measuring first pass extraction and flow with rubidium-82 in the kidneys. *Am J Physiol Imag* 5:133–140, 1990
25. HUANG SC, SCHWAIGER M, CARSON RE, CARSON J, HANSEN H, SELIN C, HOFFMAN EJ, MACDONALD N, SCHELBERT HR, PHELPS ME: Quantitative measurement of myocardial blood flow with oxygen-15 water positron computed tomography: An assessment of potential and problems. *J Nucl Med* 26:616–625, 1985
26. ROSENSPIRE KC, SCHWAIGER M, MANGNER TJ, HUTCHINS GD, SUTORIK A, KUHL DE: Metabolic fate of [^{13}N] ammonia in human and canine blood. *J Nucl Med* 31:163–167, 1990
27. GERMANO G, CHEN BC, HUANG SC, GAMBHIR SS, HOFFMAN EJ, PHELPS ME: Use of the abdominal aorta for arterial input function determination in hepatic and renal PET studies. *J Nucl Med* 33:613–620, 1992
28. HOLLENBERG NK, MANGEL R, FUNG HYM: Assessment of intrarenal perfusion with radioxenon: A critical review of analytical factors and their implications in man. *Sem Nucl Med* 6:193–216, 1976
29. HOLLENBERG NK: Renal disease, in *The Microcirculation in Clinical Medicine*, edited by WELLS R, Academic Press, New York, London, 1973, pp 61–80
30. LADEFOGED J, PEDERSEN F: Renal blood flow, circulation times and vascular volume in normal man measured by the intraarterial injection—external counting technique. *Acta Physiol Scand* 69: 220–229, 1967